N72-11328

SPACE RESEARCH COORDINATION CENTER

UNIVERSITY of PITTSBURGH 1787 VERITAS ET VIRTUS

TWILIGHT AND NIGHTTIME IONOSPHERIC TEMPERATURES FROM OXYGEN λ 6300 AND λ 5577 SPECTRAL LINE PROFILES

BY

W. A. FEIBELMAN, R. D. HAKE, JR., D. P. SIPLER

AND M. A. BIONDI

SRCC REPORT NO. 159

UNIVERSITY OF PITTSBURGH

PITTSBURGH, PENNSYLVANIA

The Space Research Coordination Center, established in May, 1963, has the following functions: (1) it administers predoctoral and postdoctoral fellowships in space-related science and engineering programs; (2) it makes available, on application and after review, allocations to assist new faculty members in the Division of the Natural Sciences and the School of Engineering to initiate research programs or to permit established faculty members to do preliminary; work on research ideas of a novel character; (3) in the Division of the Natural Sciences it makes an annual allocation of funds to the interdisciplinary Laboratory for Atmospheric and Space Sciences; (4) in the School of Engineering it makes a similar allocation of funds to the Department of Metallurgical and Materials Engineering and to the program in Engineering Systems Management of the Department of Industrial Engineering; and (5) in concert with the University's Knowledge Availability Systems Center, it seeks to assist in the orderly transfer of new space-generated knowledge in industrial application. The Center also issues periodic reports of space-oriented research and a comprehensive annual report.

The Center is supported by an Institutional Grant (NsG-416) from the National Aeronautics and Space Administration, strongly supplemented by grants from the A. W. Mellon Educational and Charitable Trust, the Maurice Falk Medical Fund, the Richard King Mellon Foundation and the Sarah Mellon Scaife Foundation. Much of the work described in SRCC reports is financed by other grants, made to individual faculty members.

Twilight and Nighttime Ionospheric Temperatures from Oxygen λ6300 and λ5577 Spectral Line Profiles

(Journal of Geophysical Research)

W. A. Feibelman, R. D. Hake, Jr., D. P. Sipler and M. A. Biondi
Department of Physics, University of Pittsburgh
Pittsburgh, Pa.

September 1971

Twilight and Nighttime Ionospheric Temperatures from Oxygen λ6300 and λ5577 Spectral Line Profiles

W. A. Feibelman†, R. D. Hake, Jr.*, D. P. Sipler and M. A. Biondi

Physics Dept., University of Pittsburgh

Abstract

Fabry-Perot interferometer measurements of atomic oxygen λ6300 and λ5577 line profiles from twilight and nightglow are used to determine the neutral temperatures in the F_2-and E-regions of the earth's ionosphere. The exospheric temperatures $T_n(\infty)$ determined from the λ6300 profiles are usually somewhat higher than those calculated from Jacchia's model, with differences as large as ~ 300°K noted when $T_n(\infty)$ = 1500 - 1600°K. The post-sunset and pre-dawn rate of change of $T_n(\infty)$ is often substantially larger than the Jacchia prediction. The λ5577 (E-region) measured temperatures range from 200-220°K on quiet nights to 500-600°K during geomagnetic storms.

†Now at Goddard Space Flight Center, Greenbelt, Md.

*Now at Stanford Research Institute, Menlo Park, California.

Twilight and Nighttime Ionospheric Temperatures from Oxygen λ6300 and λ5577 Spectral Line Profiles

W. A. Feibelman†, R. D. Hake, Jr.*, D. P. Sipler and M. A. Biondi

Physics Dept., University of Pittsburgh

I. Introduction

In recent years Fabry-Perot interferometers have gained wider application in studies of the profiles of spectral lines emitted by excited atoms in various regions of the earth's ionosphere [Hernandez and Turtle, 1965; Hilliard and Shepherd, 1966; Jarrett and Hoey, 1966; Biondi and Feibelman, 1968, Armstrong, 1968; Hays, et al, 1969]. Profiles of the OI λ5577 (green) line emitted from auroras and nightglow have provided a measure of the temperature of the neutral atmosphere at altitudes between ~ 95 and 140 km under normal and disturbed ionospheric conditions [Hernandez and Turtle, 1965; Hilliard and Shepherd, 1966]. Similarly, profiles of the OI λ6300 (red) line emitted from twilight and nightglow provide reliable determinations of the neutral atom temperature at the ~ 250-300 km level [Biondi and Feibelman, 1968 and Hays, et al, 1969] and thus give us a ground-based means of determining short and long-term variations of the exospheric temperature for comparison with models of the response of the exosphere to solar energy inputs [Jacchia, 1965].

The program of twilight and nightglow spectral line shape studies [Biondi and Feibelman, 1968] has been continued using Fabry-Perot interferometers of improved resolving power. This paper presents the results

---

†Now at Goddard Space Flight Center, Greenbelt, Md.

*Now at Stanford Research Institute, Menlo Park, California.

of our additional determinations of exospheric temperatures from λ6300 line profiles and compares them with the predictions of Jacchia's model [Jacchia, 1965]. Some information on temperatures at the ~ 100 km height level have also been obtained from λ5577 observations.

II. Experimental Apparatus

Two Fabry-Perot (F-P) interferometers of aperture 45 mm and 100 mm and of substantially higher resolution than that of our previous etalon [Biondi and Feibelman, 1968] have been employed in the present studies. The plates of the 45 mm aperture F-P, after coating with multilayer dielectric reflecting films, are flat to ~ λ/65, while the 100 mm aperture plates with reflecting coatings are flat to ~ λ/45. These latter plates have a rather high (6:1) diameter-to-thickness ratio, leading to degradation of flatness (sag defect) when mounted with their axes vertical.

As in the earlier apparatus [Biondi and Feibelman, 1968], the interferometers are operated in a pressure scanned, photoelectric detection mode in which the F-P plates are contained in a pressure-tight, thermally-insulated housing and the concentric ring interference pattern is imaged by a lens on a plate containing a small aperture centered on the pattern (see Fig. 1). Thus, a portion of the radiation constituting the central spot of the pattern passes through the aperture to the detecting photomultiplier. The wavelength corresponding to constructive interference at the central spot is made to change linearly with time by admitting argon gas to the pressure housing at a constant rate, with a consequent change in the index of refraction of the medium between the plates.

The method of determining a spectral line profile is as follows. The particular line under study, λ6300 or λ5577, is isolated from the rest of the airglow spectrum by a narrow band interference filter (10A half-width) placed either just ahead of the F-P, as shown in Fig. 1, or just before the aperture to the photomultiplier. The spectral line is cyclically scanned under the control of a master crystal clock, which starts a record cycle by closing the high conductance vent valve connected to the pressure housing. Since argon gas from the high pressure tank flows through the needle valve and into the housing at a constant rate, there is a consequent buildup of pressure in the housing (which is monitored by a pressure transducer). After the crystal clock has counted for a preset interval (typically 30-50 seconds) it opens the high conductance valve to vent the argon back to ambient pressure, resetting the cycle.

The output photomultiplier is usually operated in a pulse counting mode, its output passing through a preamplifier, discriminator, and pulse-shaping circuit. The shaped pulses from the output photomultiplier are fed into a multichannel analyzer, whose channel dwell time (typically 0.4-1 sec) and advance rate are controlled by an internal crystal clock. The start of the channel advance occurs when the argon pressure in the housing reaches a predetermined level, as monitored by the pressure transducer. Thus, it is possible to add many line scans to the memory of the multichannel analyzer (100 channel capacity) by repeating the pressure scan cycle as often as desired. We monitor the quality of the line produced by this summation process by means of an x-y point plotting chart recorder whose y axis is driven by the analogue output of the analyzer and whose x axis is driven by the voltage output from the pressure transducer. When a sufficient number of line scans have been stored in the memory to produce a satisfactory line profile, the counts in each channel are printed out by the digital printer.

A separate monitor photomultiplier records the total line intensity emitted from the same region of the sky (but from a solid angle of $\sim 10^{-5}$

steradians) as observed by the Fabry-Perot (solid angle, $\sim 10^{-6}$ steradians) by monitoring the signal passing through the interference filter and reflecting from the input window of the pressure housing. To calibrate the F-P, the overall instrumental broadening is determined by means of a narrow spectral line of known width from either an r-f excited isotopic mercury source ($\lambda 5461$) or from a frequency stabilized helium-neon laser ($\lambda 6328$).

III. Determination of Line Shapes and Widths

The recorded spectral line profiles consist of a convolution of the actual line profile and the instrumental broadening factors. In the reduction of the data we have assumed for simplicity that the actual line profile can be adequately represented by a sum of gaussian profiles. The instrumental broadening factors have been separated into three parts; (a) finite reflecting finesse, N_R (i.e. $R < 1$), whose broadening effect is represented by the Airy function, (b) finite flatness (defect) finesse, N_D, represented by either a spherical deviation from absolute plate flatness, a random deviation (gaussian distribution) from parallelism [Chabbal, 1958], or both and (c) finite aperture finesse, N_A, due to finite size of the exit plane aperture. Following Hernandez [1966], we represent the Airy function as a Fourier series and convolve Airy, defect, and aperture functions to obtain expressions for the coefficients a_n of a cosine series which represents this convolution. Similarly, when a gaussian spectral line shape is convolved with the Airy, defect, and aperture functions, expressions are obtained for the coefficients b_n of the cosine series which represents this overall convolution. By this method we can synthesize the spectral line profile to be expected when a thermal doppler (gaussian) line is observed with the Fabry-Perot.

In analyzing a line profile in detail, a computer is used to fit the measured data points representing the line shape to a cosine series. In this process it is found that, as a result of scatter in the data, the coefficients c_n of the series exhibit large and random variations for too high a harmonic (e.g. $n > 10$); thus the fitting process is carried out with a series terminated at the appropriate n value.

To analyze the bulk of the data, a simplified procedure has been adopted which is based on the assumption that the actual spectral line is close to gaussian in form. By means of the convolution schemes discussed earlier, graphs are constructed of emitting atom temperature (in effect, doppler half-width) as a function of the observed contrast finesse (i.e., free spectral range divided by line width measured at an intensity midway between maximum and minimum in the observed line tracing) with instrumental finesse as a parameter. In this way the λ6300 and λ5577 line profile data can be analyzed to obtain atom temperatures without lengthy computer fitting of each profile. The deduced temperatures are somewhat sensitive to the assumed form of plate defect - spherical or random - leading to possible systematic errors which have been included in our estimate of the uncertainties in the derived temperatures. In fitting the observed λ6300 and λ5577 profiles, we find that the temperature inferred assuming a purely spherical plate defect is up to 60°K higher than that obtained assuming a purely random defect. In actuality, the aligned F-P plates exhibit a rather complex defect pattern, much of which results from hill - and - valley deviations from flatness.

Fortunately, any systematic error which is present remains the same throughout a given night. Thus, the deduced variations in temperature are much more accurate than are the absolute temperature values, whose uncertainties are indicated by the error bars in Figs. 2-4.

IV. Experimental Observations

The observations reported in this paper were made at the University of Pittsburgh's Airglow Observatory at Laurel Ridge, Pa. (40° 10'N., 79° 10'W.) and cover the period June 9, 1968 to September 13, 1969. Those made up to July 20, 1968 were obtained with the 45 mm aperture interferometer typically operating at an overall instrumental finesse of ~ 18 with an 11 mm spacer. Those made following that date were made with the 100 mm aperture interferometer, operating first with the axis of the F-P plates vertical and therefore at a reduced finesse (~ 13) due to sag defect and later (after Feb. 1969) with the plates' axis horizontal (overall finesse ~ 18). The spacers used were either 5 mm or 10 mm. The dates on which λ6300 and/or λ5577 line profiles were obtained during the twilight and night are given in Table 1 (together with the measured green line temperatures). Unless otherwise noted on the figures which follow, the observing direction was WNW in azimuth and at 30° elevation.

The results for two summer nights are shown in Figs. 2 and 3, where T_{FP} represents the oxygen atoms' temperature at ~ 250 km and ~ 100 km deduced from the half widths of the red and green line profiles obtained with the Fabry-Perot interferometer. The time is Eastern Standard Time (0000 EST = 0500 UT), and the error bars on the figures represent our estimate of both random and systematic errors; the former are largely determined by the quality of the line profiles, while the latter depend on the actual form of the plate defect (as opposed to the idealized models assumed in the analysis). The dashed curve labelled T_J is the temperature variation calculated using the empirical model of Jacchia [1965] relating exospheric heating to values of the 10.7 cm solar flux $F_{10.7}$ and of the planetary magnetic index K_p. The data of July 29-30 indicate a much stronger fall following sunset and a much sharper rise at dawn than predicted by Jacchia's model. (The observing azimuth was changed from WNW to NE at 0150 to take advantage of the post-sunset and pre-dawn twilight enhancements in the red line intensity.) The green line apparent temperatures were approximately 210°K on both June 21-22 and July 29-30, although a slight fall and rise may be indicated in the June 21-22 data.

The form of the red line temperature variation changes from night to night, as may be seen from an examination of Figs. 2, 3, and 4. In order to compare our λ6300 temperature observations over a long period of time with the temperatures predicted by Jacchia's empirical model we have plotted the interferometrically observed values T_{FP} (obtained on the nights listed in Table I) against the model values T_J in Fig. 5. (In many cases several of the values measured within a short period of time have been averaged together and plotted as a single point to avoid crowding on the figure). Taken as a whole, the observed temperatures appear to lie slightly higher (~ 200°K) than the predicted values.

Inasmuch as most of our observations shortly after sunset suggest an initially higher observed temperature which then falls faster than the model prediction, we have divided the data points in Fig. 5 into those obtained in the early night, ~ 2 hours after local ground sunset (circles), and those obtained 2-3 hours later (triangles) and replotted them in Fig. 6. It will be seen that, while observed and predicted temperatures seem to be in agreement in the 1000-1100°K range, in the early night when higher temperatures are often noted the measured temperatures are consistently higher than the predicted values (with the exception of the open symbols representing March 1969 data which are also shown in Fig. 4). The data more nearly follow the steeper dashed line than the solid line at slope = 1.

The data on green line apparent temperatures for the same period are summarized in Table I. On most nights a temperature in the vicinity of 210°K is indicated by the more accurate runs (± 50°K error); however on a few occasions much higher temperatures, 500-600°K, are indicated, a notable case occurring on November 2, 1968, one day after a widespread red line aurora associated with an intense geomagnetic storm was visible from the observatory.

V. Discussion and Conclusions

A. λ6300 Observations

The λ6300 line profile measurements provide information concerning the exospheric temperature $T_n(\infty)$ and its variation over the post-sunset to pre-dawn period. In some respects the measurements of T_{FP} are more readily related to $T_n(\infty)$ than are T_i and T_e determinations obtained from incoherent backscatter measurements. It has been shown [Biondi and Feibelman, 1968] that, even though the $O(^1D)$ excited oxygen atoms are produced dissociatively with excess kinetic energy, at the ~ 250-300 km altitude usually associated with red line emission the atoms are thermalized before radiating and so emit a thermal doppler profile characteristic of the ambient temperature. For the lower emission altitude (~ 250 km) this ambient temperature is slightly smaller (~ 100°K) than the exospheric temperature; thus the measured red line temperatures T_{FP} are slightly smaller than or equal to $T_n(\infty)$. In the case of the backscatter observations [Hays, et al, 1970; Cogger, et al, 1970; Swartz and Nisbet, 1971; McClure, 1971; McClure and Troy, 1971] the measurements of T_e and/or T_i yield upper limits to $T_n(\infty)$, inasmuch as elevation of T_e and sometimes even T_i above T_n may occur at night. However, intercomparison of T_{FP} and backscatter T_i or T_e values [Hays, et al, 1970; Cogger, et al, 1970] have shown that under appropriate conditions the optical and radar determinations agree within the combined experimental uncertainties.

The observations reported in the present paper generally confirm the previous optical interferometer and backscatter measurements in finding that the Jacchia model provides a rough prediction of the exospheric temperature. However, the solar and geomagnetic indices used in the empirical model do not seem to account properly for the changes in $T_n(\infty)$ observed over the span of a few days. Further, the diurnal variation predicted by the Jacchia model is usually substantially weaker than the observed variation of $T_n(\infty)$ - see Figs. 2 and 3 of the present paper and Figs. 1 and 5 of Waldteufel and Cogger [1971]. When changes in the K_p values are small, Jacchia's model (either the 1965 model used in the present paper or the more recent 1970 model [Jacchia, 1970]) predicts a post-sunset fall of temperature of the order of 30°K/hr. Temperature decreases of ~ 60°/hr have been reported for interferometric [Roble et al, 1970] and backscatter observations [Waldteufel and Cogger, 1971]. In the present case the July 29-30, 1968 data of Fig. 3 indicate an even stronger fall of ~ 200°/hr. well after sunset and a comparably sharp rise before dawn. It is difficult to see how the empirical model should be modified to account for these rapid changes.

The Jacchia model appears to be most deficient in predicting the occurrence of the higher exospheric temperatures (1500-1600°K). As may be seen from Figs. 5 and 6, the Jacchia model temperatures appear to be ~ 300°K lower than the observations. Also rather puzzling are the data of March 13 and 22, 1969 (see Fig. 4) where the measured temperature starts from the vicinity of the model temperature T_J after sunset and then falls substantially below the model prediction. It is possible that the peak emission altitude on these nights was rather low, so that $T_{FP} < T_n(\infty)$. However, we have previously observed red line temperatures substantially smaller than the predicted T_J values; on October 12, 1966 a value $T_{FP} \simeq 650°K$ was observed when the predicted exospheric temperature value was $T_J \simeq 1000°K$ [Biondi and Feibelman, 1968]. In both the present observations and the earlier ones, it is difficult to account for so large a difference between T_{FP} and $T_n(\infty)$ for any reasonable lowering of the altitude of peak red line emission.

An interesting comparison of our red line temperature measurements with those of Roble et al [1970] can be made for the evening of October 30, 1968, some 5 hours before the occurrence of a SAR arc. On that evening we were engaged chiefly in green line measurements, but at 1910 and at 1957 EST temperatures of (1620 $\pm$ 200) and (1350 $\pm$ 200)°K, respectively, were obtained from red line profiles with substantial statistical fluctuations in the data points. These values are substantially higher than observed from the Michigan Airglow Observatory at Ann Arbor where at 2000 and 2040 EST Roble, et al reported values of $\sim$ 1000°K. Our observing direction, 30° elevation WNW, intersected the ionosphere at 250 km slightly south of the zenith at Ann Arbor; thus we should have expected closer agreement with the Michigan data. If the Michigan observations were made in the zenith over Ann Arbor, it is possible that the difference in the apparent temperatures could have resulted from horizontal winds with a velocity gradient or shear through the emitting layer. Thus, our λ6300 profiles observed at 30° elevation angle would have been broadened relative to the Michigan observations. Recently, Hays and Roble [1971] reported that on the following night, October 31, doppler shifts in the λ6300 line position indicated a north-south wind of $\sim$ 200-300 m/sec during a SAR arc. In the past we have observed a west-to-east component of wind from shifts in the λ6300 line position [Biondi and Feibelman, 1968].

High exospheric temperatures were also observed from Laurel Ridge on November 2, 1968 (during an intense geomagnetic storm), when over the period 1812 to 2016 EST red line temperatures between 1500 and 1600°K were measured. However, on this night consistently high green line temperatures (~ 580°K) were noted both to the north and to the west (see Table I), suggesting widespread particle precipitation, although no visual sightings of auroral activity were noted in the log.

B. λ5577 Observations

Although the interferometer was more nearly optimized for accurate determinations of the red line rather than the green line apparent temperatures, a significant part of our observations were devoted to λ5577 line profile measurements. The quoted temperature accuracy for our better runs (~ ± 50°K) is considerably poorer than that quoted by Hernandez and Turtle [1965] and by Armstrong [1968]; however we have included a possible systematic error resulting from differences between the actual plate defect and the idealized defect forms assumed in the analysis. During the 1968-1969 observed period we observed a maximum λ5577 intensity on quiet nights during late autumn (October) and a minimum four months later (February), just six months out of phase with the southern hemisphere observations reported by Armstrong [1968].

Our quiet night observations suggest green line minimum temperatures of 200-220°K (see Table I), in good agreement with the 1964-1965 (solar minimum) results of Hernandez and Turtle [1965]. However, our measurements disagree with Armstrong's results obtained at solar minimum which indicated mean values of 155°K in January, rising to 200°K in April, and falling to 170°K in August. On the basis of temperatures from the U.S. Std. Atmospheres Suppl., 1966, our observations place the peak of the λ5577 emitting layer at ~ 95 km in winter and at ~ 103 km during the other seasons.

Our measurements of obviously elevated apparent temperatures on nights such as September 7, October 23, November 2 and November 21, 1968 and on February 5, 1969 (see Table I) were often correlated with observation of brightening of some portion of the night sky, suggesting auroral activity. In those data where the quoted uncertainties are not too large, e.g., November 2 and 21, the spectral line shapes appeared to be simple in form. That is, they did not appear to be a superposition of a low temperature gaussian (E layer origin) and a high temperature gaussian or a dissociative line profile (F layer origin), the sum of which gave an increased line width and an apparently higher temperature than the E region temperature (see, for example, the analysis of Hays and Walker [1966] and the observations of Hernandez [1971]). Thus, these elevated temperature lines were evidently produced at higher altitudes, ~ 135 km for 580°K and ~ 128 km for 450°K (U.S. Standard Atmosphere Supplements, 1966), as a result of auroral activity in the form of relatively soft particle precipitation. For those elevated temperatures with large uncertainties, such as September 7, 1968, the statistics in the line profile measurements are not good enough to rule out contamination of a narrow E layer line profile with a broader F layer component. In future studies we shall obtain simultaneous measurements of the red line and the green line profiles in order to evaluate possible "contamination" of the λ5577 profiles by radiation originating in the F region.

As may be seen from the data of June 21-22, 1968 (Fig. 2) there is some evidence that on an apparently quiet night the green line temperature falls from an initial value at 2300 EST of ~ 220°K to a value of ~ 160°K at 0200 EST. While the data of July 29-30 (Fig. 3) suggest that such a diurnal variation is not always to be expected, it should be noted that many of the green line temperatures given in Table I refer to averages obtained from pre-midnight determinations and thus may not be representative of the all-night average value.

Acknowledgements

The authors wish to thank M. A. Stoenescu for assistance in reduction of the line profile data. This research has been supported, in part, by the National Science Foundation, Atmospheric Sciences Division (Aeronomy), GA-18224.

Table I. Observing dates and green line temperatures.

Yr.	Mo.	Day	$T_{FP}[\lambda 5577]$ (°K)	Yr.	Mo.	Day	$T_{FP}[\lambda 5577]$ (°K)
1968	June	9	220 ± 50	1968	Oct.	8	170 ± 100
		21-22	200 ± 50			13	240 ± 40 (2040)*
		29	250 ± 70				to 320 ± 50 (2110)
	July	4	200 ± 50			15	220 ± 40
		15	210 ± 70			21	240 ± 50
		29-30	215 ± 40			23	450 ± 100
	Aug.	11	150 ± 100			30	240 ± 60
		12	200 ± 100		Nov.	2	580 ± 100
		14	---			21	450 ± 80 (1820)
		15	180 ± 120				to 310 ± 80 (1945)
		28	250 ± 100	1969	Feb.	5	400 ± 150
	Sept.	7	540 ± 200			18	---
		20	230 ± 40		March	4	---
		26	250 ± 50			13	---
						22	320 ± 100
					Sept.	13	---

*Quantities in parentheses are EST.

References

Armstrong, E. B., Variations in the width of the OI λ5577 line in the night airglow, Planet. Space Sci., 16, 211, 1968.

Biondi, M. A. and W. A. Feibelman, Twilight and nightglow spectral line shapes of oxygen λ6300 and λ5577 radiation, Planet. Space Sci., 16, 431, 1968.

Chabbal, R., Finesse limite d'un Fabry-Perot forme de lames imparfaites J. Phys. Radium 19, 295, 1958.

Cogger, L. L., G. J. Nelson, M. A. Biondi, R. D. Hake, and D. P. Sipler, Coincident F-region temperature determinations from incoherent backscatter and doppler broadening of [OI]6300A, J. Geophys. Res. 75, 4887, 1970.

Hays, P. B. and R. G. Roble, Direct observations of thermospheric winds during geomagnetic storms, J. Geophys. Res., 76, 5316, 1971.

Hays, P. B. and J. C. G. Walker, Doppler profiles of the 5577A airglow, Planet. Space Sci., 14, 1331, 1966.

Hays, P. B., A. F. Nagy and R. G. Roble, Interferometric measurements of the 6300A doppler temperature during a magnetic storm, J. Geophys. Res., 74, 4162, 1969.

Hays, P. B., A. F. Nagy, K. D. McWatters, and J. V. Evans, Comparison of radar and optical temperature measurements in the F region, J. Geophys. Res., 75, 4881, 1970.

Hernandez, G., Analytical description of a Fabry-Perot photoelectric spectrometer, Appl. Opt., 5, 1745, 1966.

Hernandez, G., The Signature Profiles of $O(^1S)$ in the airglow, Planet. Space Sci., 19, 467, 1971.

Hernandez, G. J. and J. P. Turtle, Nightglow 5577A [OI] line kinetic temperatures, Planet. Space Sci., 13, 901, 1965.

Hilliard, R. L. and G. G. Shepherd, Upper atmospheric temperatures from doppler line widths-IV, Planet. Space Sci., 14, 383, 1966.

Jacchia, L. G., Static diffusion models of the upper atmosphere with empirical temperature profiles, Smithson. Contrib. Astrophys., 8, 215, 1965.

Jacchia, L. G., New static models of the thermosphere and exosphere with empirical temperature profiles, Smithson. Astrophys. Obs. Spec. Rep., 373, 1970.

Jarrett, A. H. and M. J. Hoey, Observations of the 6300A OI nightglow emission, J. Atmos. Terr. Phys., 28, 175, 1966.

McClure, J. P., Thermospheric temperature variations inferred from incoherent scatter observations, J. Geophys. Res., 76, 3106, 1971.

McClure, J. P. and B. E. Troy, Equatorial ion temperature: a comparison of conflicting incoherent scatter and OGO-4 retarding potential analyzer values, J. Geophys. Res., 76, 4534, 1971.

Roble, R. G., P. B. Hays, and A. F. Nagy, Photometric and interferometric observations of a mid-latitude stable auroral red arc, Planet. Space Sci., 18, 431, 1970.

Swartz, W. E. and J. S. Nisbet, Diurnal variation of the neutral temperature profile at Arecibo from incoherent scatter measurements and its relevance to the 1400 - hour density maximum, J. Geophys. Res., 76, 185, 1971.

Waldteufel, P. and L. Cogger, Measurements of the neutral temperature at Arecibo, J. Geophys. Res., 76, 5322, 1971.

Figure Captions

Fig. 1 Simplified diagram of the Fabry-Perot interferometer apparatus.

Fig. 2 Interferometrically determined red and green line temperatures of June 21-22, 1968. The dashed line represents the Jacchia [1965] model predictions.

Fig. 3 Interferometrically determined red and green line temperatures on July 29-30, 1968.

Fig. 4 Red and green line temperatures on August 12, 1968 and March 13 and 22, 1969. The observing direction on August 12 and March 13 is WNW.

Fig. 5 Comparison of interferometrically determined red line temperatures with the predicted exospheric temperatures using Jacchia's [1965] model. The data are for the observing dates listed in Table I.

Fig. 6 Separation of the data shown in Fig. 5 into early night (~ 2 hours after local ground sunset) and later night (2-3 hours later) components. The solid lines at unit slope would be followed if the T_{FP} and the T_J values were in agreement.

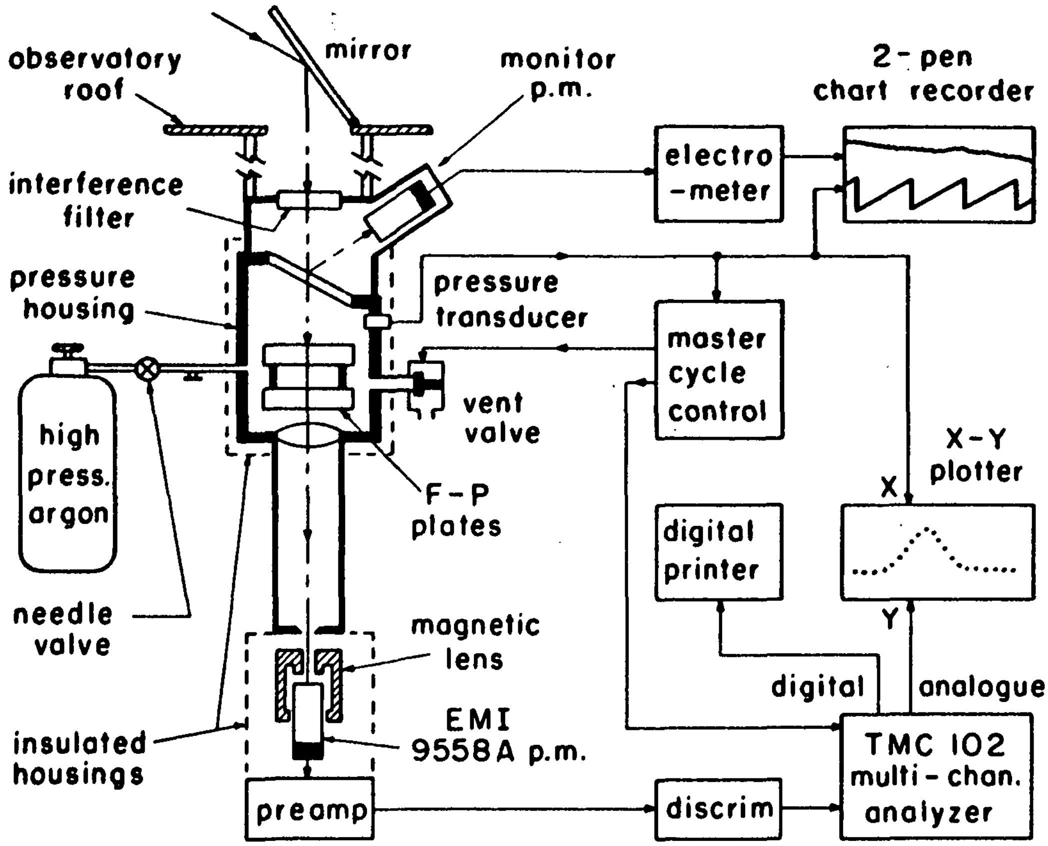

Figure 1

Simplified diagram of the Fabry-Perot interferometer apparatus.

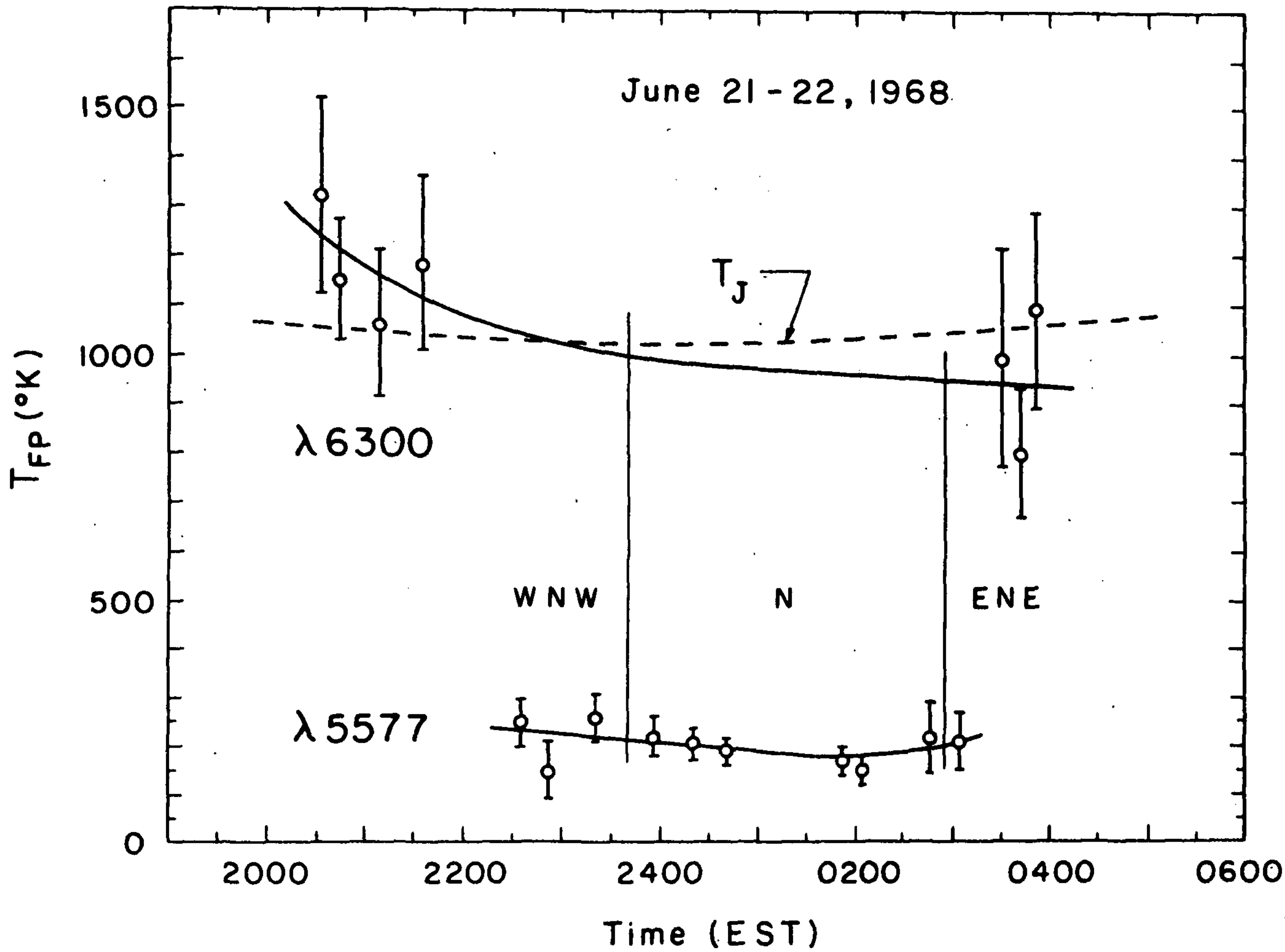

Figure 2

Interferometrically determined red and green line temperatures of June 21-22, 1968. The dashed line represents the Jacchia [1965] model predictions.

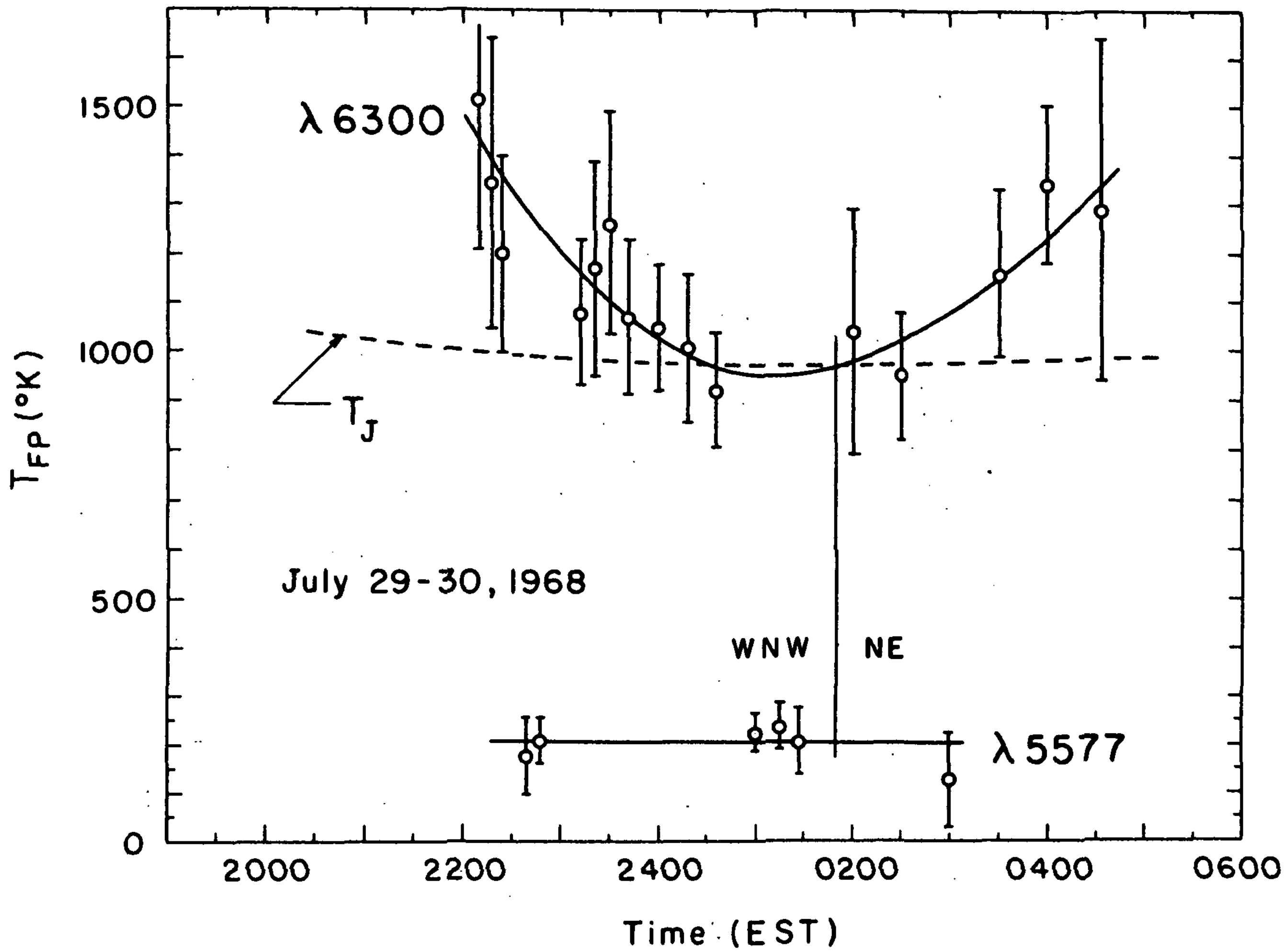

Figure 3

Interferometrically determined red and green line temperatures on July 29-30, 1968.

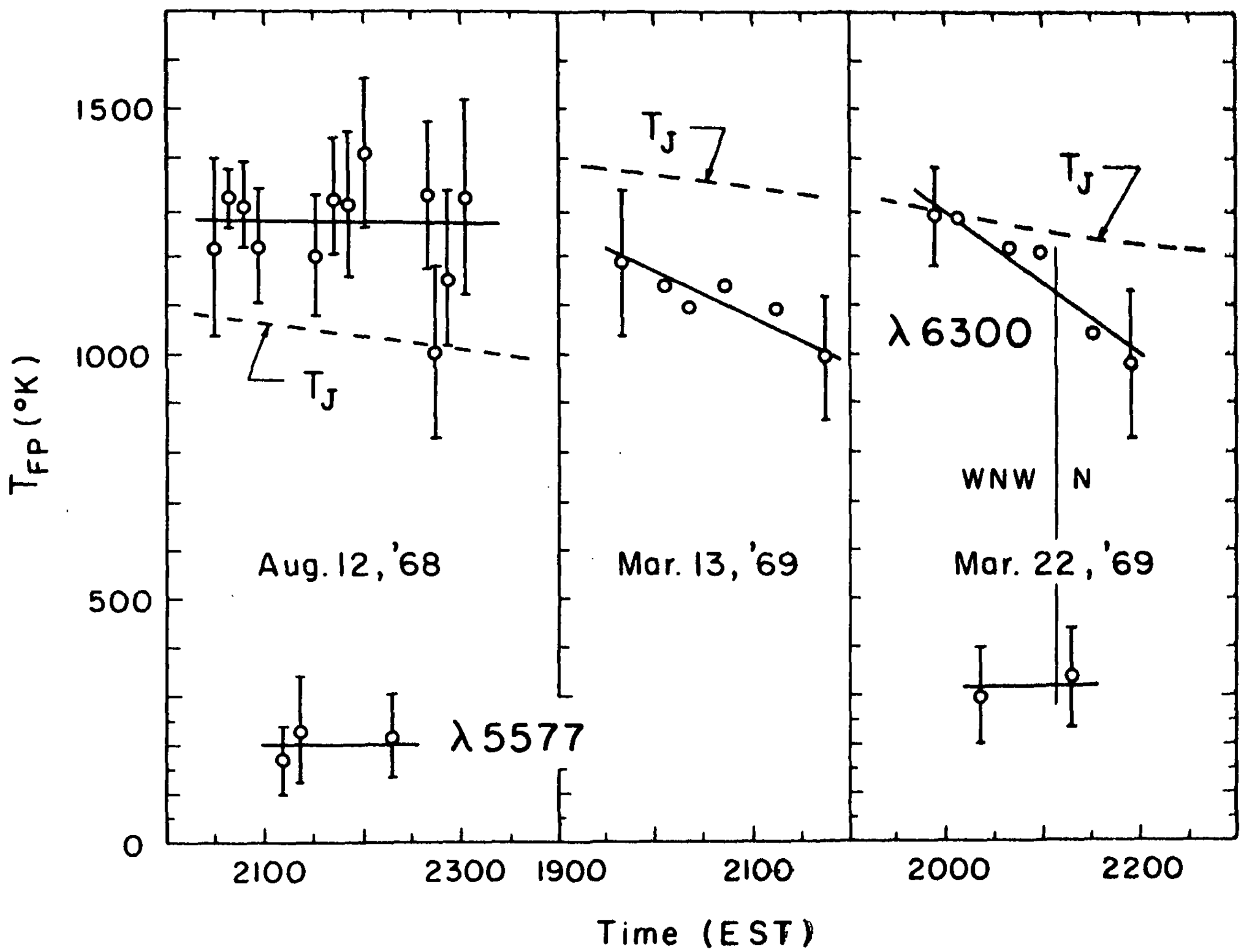

Figure 4

Red and green line temperatures on August 12, 1968 and March 13 and 22, 1969. The observing direction on August 12, and March 13 is WNW.

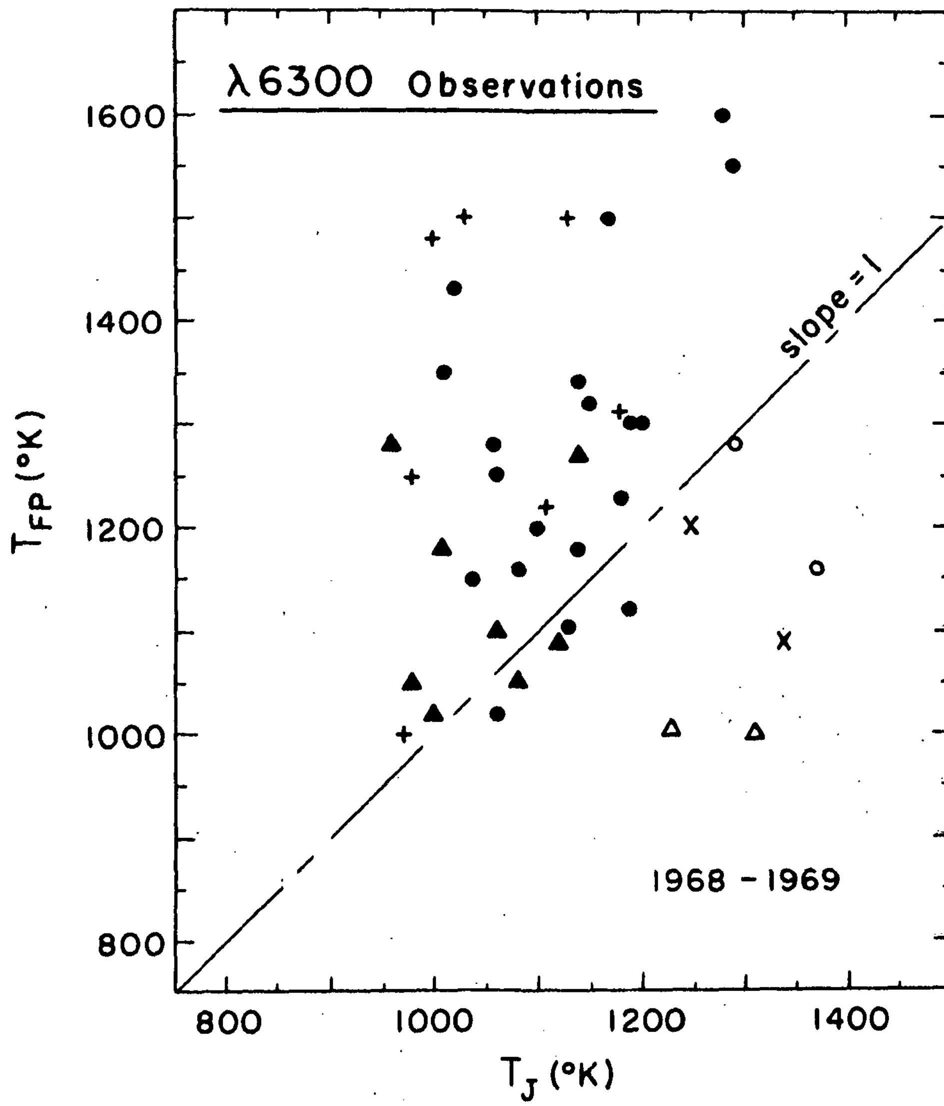

Figure 5

Comparison of interferometrically determined red line temperatures with the predicted exospheric temperatures using Jacchia's [1965] model. The data are for the observing dates listed in Table I.

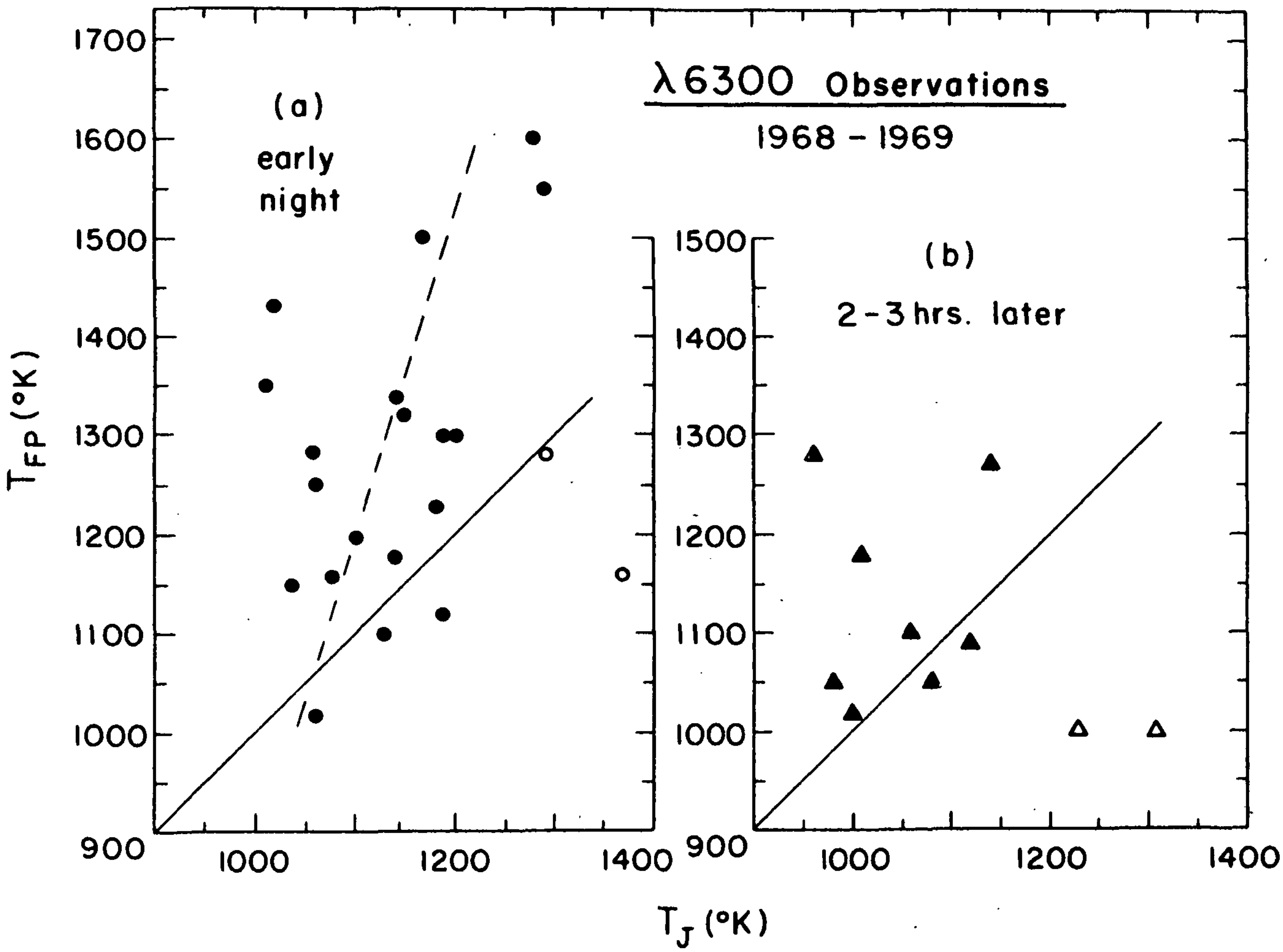

Figure 6

Separation of the data shown in Fig. 5 into early night (~ 2 hours after local ground sunset) and later night (2-3 hours later) components. The solid lines at unit slope would be followed if the T_{FP} and the T_J values were in agreement.